Rend. Sem. Mat. Univ. Politec. Torino
Vol. 68, 4 (2010), 397 – 411

G. Lauro, M. Lisi and R. Monaco

A MODELING FRAMEWORK FOR ANALYSIS OF LANDSCAPE STABILITY AND BIFURCATION PHENOMENA

Abstract. In the framework of Landscape Ecology, we propose an integrated approach that combines an ecological graph model for the analysis of the relationship between spatial pattern and ecological flows and a mathematical model, based on a system of two nonlinear differential equations that studies landscape stability and bifurcation phenomena. A case study of the district of Cremona (Italy) is performed, and this furnishes some threshold values of the graph connectivity index corresponding to bifurcations between two possible different equilibrium states.

1. Introduction

Landscape Ecology [11, 8] is an interdisciplinary field that needs reciprocal integration between theoretical developments and empirical testing and applications. In this framework, landscapes can be defined as spatially extended heterogenous complex systems organized hierarchically into structural arrangements determined by nonlinear interactions among their components through flows of energy and materials. Moreover, they are far from equilibrium and meta-stable, that is, landscapes respond stably only over a limited range of conditions but may eventually undergo significant alterations if environmental constraints continue to change, giving rise, possibly, to bifurcation phenomena [9]. In this context, simulation models are becoming powerful tools to view and analyze the nonlinear dynamics of such systems with the aim to furnish information on their trend toward possible future scenarios.

In this paper we propose two interconnected models that integrate spatial and temporal analysis. The first one, static, uses Landscape Ecology's tools and deals with an ecomosaic model of the territory, under investigation, as composed by several landscape units, i.e., connected patches of ecotopes. These units are separated from each other by anthropic or natural barriers (for example, roads or rivers). Hence, by means of a Geographic Information System software (GIS), we construct a planar graph overlapped to the ecomosaic, the so-called Ecological Graph (EG), where the nodes are circles whose area is proportional to the magnitude of Biological Territorial Capacity (BTC), defined as the energy ($Mcal/m^2/year$) required by a system to maintain its equilibrium state and its organizational level [6]. This value, as shown in the sequel, is made up of the energy contributions given by different ground uses (ecotopes) present in each unit. Moreover, in this model, graph edges have thickness proportional to energy flux between two consecutive land units: the more will be the permeability of the barriers the more will be the thickness of edges. Hence, such a graph exhibits a picture of current ecological health's state of the landscape, also with regard to its level of fragmentation.

The second model, dynamical, studies the evolution in time of such a state by means of a system of two nonlinear differential equations where one of the two unknowns, named "bio-energy", is linked to the average BTC over the whole ecomosaic and the other one gives the percentage of land characterized by high value of bio-energy (for example, wooden areas). Hence, meta-stability can be investigated by means a stability analysis of equilibrium solutions of such a dynamical system together with the analysis of possible bifurcation phenomena, appearing when the parameters involved in the equations reach critical thresholds.

The two models, static and dynamic, are interconnected because the variables definitions and the parameters involved in the differential equations are technically linked to the quantities calculated in the EG, as will be shown in the next section. Then, the paper is organized as follows. In Section 2 we give definitions and tools to construct the EG relative to a given landscape and we propose a coupled system of two nonlinear differential equations. They are mainly based on a balance law between a logistic growth of the two above mentioned state variables against their decrease due to limiting factors coming from environmental constraints. In Section 3 we find the equilibrium solutions of such a dynamical system and study their stability. Moreover, we evaluate the bifurcation values of a significant parameter of the equations, the “connectivity”, that furnishes a measure of landscape fragmentation. Finally, an Appendix is devoted to the details on all the quantities that appear in both models.

2. The Ecological Graph and the dynamical model

In the modern discipline of Landscape Ecology, landscape is defined as a heterogenous land composed of interacting ecosystems that exchange energy and matter, and where natural and anthrop events coexist. In the present model an environmental system, [3, 6], is subdivided in a given number, m, of different ecological patches (landscape units) separated from each other by natural or anthrop barriers. The energy content of each patch may be represented by a circle (node) whose diameter is proportional to the magnitude itself. The barriers can have different degrees of permeability to energy flow [6, 7]. For example, roughly speaking, a highway has zero value of permeability and determines, hence, a territorial fragmentation.

We can represent the various levels of energy connection, among the patches, by edges whose width is proportional to the energy flux shared among them. As already mentioned in the Introduction, the collection of nodes and edges is called the EG of the environmental system [3]. It can be drawn by means of a software GIS (Arch View 3.3) by using the information, contained in suitable shape files and database furnished by local government, about land uses, presence and connection of road infrastructures (railroads, highways, government and provincial roads), system of water courses (natural and artificial), ridges and administrative subdivision of the various urban territories within the studied landscape.

In Figure 1 the graph of an environmental system inside the district of Cremona (Italy), including 10 municipalities, is proposed. Here the ecomosaic is composed of eight patches all mutually linked, since none of the barriers is completely impermeable,

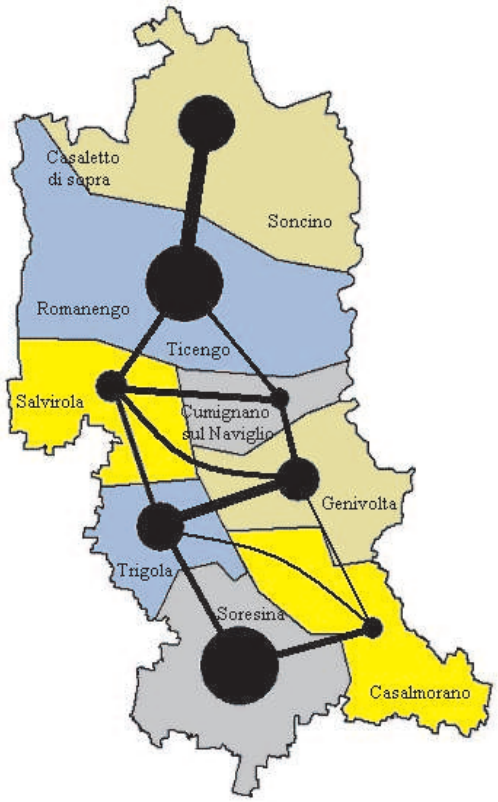

Figure 1: The ecological graph of an environmental system

but with different levels of width among its edges. For example, between Genivolta and Casalmorano units we can see a very thin edge meaning that there is a weak energy flow exchange. Moreover, the energy content of Casalmorano unit is very low as shown by the small size of its node. Hence, from the graph of Figure 1, we get the information that this area needs territorial interventions improving its ecological value furnishing, in turn, a more stable ecosystem. It is up to urban planners of the municipality to provide suitable transformations in such a direction.

The graph so obtained, represents in a static way, the distribution of energy in the territory. As said in the Introduction, we now define the bio-energy of patch j, $j = 1,\ldots,m$, by [3, 6]

$$\mathcal{M}_j = (1+K_j)B_j, \tag{1}$$

where $K_j \in [0,1]$, environmental indicator, is a dimensionless parameter characterizing the morphological features of patch j; B_j is the value of BTC computed on the basis of a standard classification [6], once the ground uses present in patch j are identified

by means of GIS. Such a classification runs from 0 to 5 $Mcal/m^2/year$, [6]: the lowest value concerning edificial (biologically non-active) areas, the maximum being relative, for example, to natural wooden areas. Namely,

$$B_j = \frac{1}{n}\sum_i^n B_{ij}^E s_{ij} \tag{2}$$

where s_{ij} is the area of ecotope i, $i = 1,\ldots,n$, the smallest ecologically distinct unit inside the patch j and where B_{ij}^E is the relative value of BTC. The parameter K_j is computed as the average between three parameters K_j^S, K_j^P, K_j^B (each with values in $[0,1]$), linked, respectively, to shape, permeability of barriers and to bio-diversity, as reported in detail in Appendix.

Once the bio-energy of each patch is computed, we can define that one of the whole system by performing the average over all the patches, i.e.

$$\mathcal{M} = \frac{1}{m}\sum_{j=1}^m \mathcal{M}_j. \tag{3}$$

Moreover, in what follows, we shall use, instead of $\mathcal{M}$, the normalized bio-energy $M = \mathcal{M}/\mathcal{M}_{\max}$, where $\mathcal{M}_{\max}$ is the maximum value of bio-energy that the environmental system under consideration can produce. The computation of $\mathcal{M}_{\max}$ is reported in the Appendix, see formula (17).

Another important quantity, peculiar of the environmental system is the ratio V between the amount of territory surface characterized by high values of BTC and the whole surface of the territory itself.

As discussed in the Introduction, the main purpose of the present paper consists in analyzing a dynamical model which considers the quantities $M(t)$ and $V(t)$ as state variables depending on time t. Some ideas how to construct such a model can be found in the book [7], where separate equations for the quantities M and V were deduced. Here we propose a coupled system of equations by the conjectures which follow.

The time evolution of bio-energy $\mathcal{M}$ will be ruled by a balance of two terms with opposite sign. The first states an increasing of energy, by following a logistic rule, i.e.

$$c\mathcal{M}(t)\left[1-\frac{\mathcal{M}(t)}{\mathcal{M}_{\max}}\right],$$

where c is the so-called connectivity index. This index, as it will be shown, plays a crucial role in the global behavior of the model. For this reason it will be chosen as the control parameter of the dynamical system. It depends essentially on the number and the width of EG edges, hence, on bio-energy fluxes between the patches of the landscape. Therefore, it takes into account the grade of permeability of the barriers, furnishing, then, a global measure of landscape fragmentation. Its precise definition and computation will be presented in the Appendix, see formulas (18) and (19).

The second term, negative, takes into account the decrease of energy due to environmental factors, and is given by

$$-hS(t)\mathcal{M}_{\max},$$

where h is the ratio between the length of the impermeable barriers, that obstruct energy passage, and the total perimeter of the environmental system; $S(t)$ is the ratio between the territory surface that, at time t, presents low value of BTC, and the total surface of the system.

According to the definition of $V(t)$, the state variable $S(t)$ can be explicitly given by $1-V(t)$; thus, by introducing the normalized bio-energy $M = \mathcal{M}/\mathcal{M}_{\max}$, the time evolution equation for M reads

$$M'(t) = cM(t)[1-M(t)] - h[1-V(t)]. \tag{4}$$

For what concerns the time evolution of $V(t)$, again we suppose that it depends on two opposite terms, a positive growth $M(t)V(t)[1-V(t)]$, where the logistic rule is weighted by the normalized bio-energy M itself (the bigger $M(t)$ the bigger growth of $V(t)$) and a negative term, $-h_R U_0 V(t)$, opposing to such a growth. Here, h_R is an environmental parameter that is defined by the ratio between the perimeter of the edified area (biologically non-active) and the total perimeter of the system; U_0 is the ratio (assumed as constant) between the surface of the edified areas and the total surface of the environmental system. Hence, the second evolution equation is given by

$$V'(t) = M(t)V(t)[1-V(t)] - h_R U_0 V(t). \tag{5}$$

In the model (4)–(5), according to their definition, the state variables M and V and the quantities c and U_0 have values in the real interval $[0,1]$, whereas the positive parameters h and h_R can take also values larger than one, marking, in this case, that the territorial settlement presents some criticality. As one can check, all of these environmental indicators are linked to the EG.

The system (4)–(5) must be supplemented with the initial data $M(0) = M_0$ and $V(0) = V_0$. Once more, these data are determined by the EG which, as we have earlier discussed, fixes at time $t = 0$ the current state of the environmental system under consideration. Thus, differential equations (4)–(5) rule the dynamical development of such a system towards future scenarios that will be analyzed in next section.

3. Stability analysis and bifurcation phenomena

It is interesting to study the equilibrium solutions of system (4)–(5), because they can give, depending on suitable values of the parameters, indications on the level of meta-stability of the model. In fact, changes in bio-energy and environmental conditions may produce territorial modifications toward which, for instance, individual landscapes may produce critical thresholds that result in radical changes in the state of the ecological system. In a simple way, as we have already underlined, we can say that meta-stability means that an ecological system can keep itself over a limited range of changes in environmental conditions but may eventually undergo significant alterations if environmental constraints continue to change. The more or less meta-stability (i.e., the more or less resistance to disturbances) is related to the more or less presence of bio-diversity and connectivity [6, 3, 9].

By setting the right-hand side of system (4)–(5) equal to zero, we obtain many kinds of equilibrium solutions.

First of all, we have the following two solutions ($M^e_1 \leq M^e_2$):

$$\begin{cases} M^e_{1,2} = \dfrac{1}{2} \pm \sqrt{\dfrac{1}{4} - \dfrac{h}{c}}, \\ \\ V^e_{1,2} = 0. \end{cases} \tag{6}$$

Obviously, the existence in the real field of such solutions requires $c \geq 4h$.

REMARK 1. This equilibrium configuration corresponds to a territorial settlement with a lack of areas at high value of biological activity ($V^e = 0$) but, the condition of low impermeability h and/or high connectivity index c, allows to have M different from zero. In fact, since $c \in [0,1]$, condition $c \geq 4h$ requires that the maximum value of h, in this case, must be less or equal to 1/4.

In order to find equilibrium solutions with V^e different from zero, it is easy to prove that we must calculate the solutions of the following third order equation:

$$M^3 - M^2 + H = 0, \qquad H = hh_R U_0/c. \tag{7}$$

The corresponding values of V^e are

$$V^e = 1 - \frac{h_R U_0}{M^e}. \tag{8}$$

REMARK 2. Note that meaningful positive values of $V^e = 1 - \dfrac{h_R U_0}{M^e}$, in $[0,1]$, correspond to values of $M^e > h_R U_0$.

We get three different sets of solutions.

Case 1. $H > 4/27$:

Equation (7) will admit two complex conjugate solutions and a unique negative real one, i.e.

$$M^e_3 = \frac{1}{3} + \left[\frac{1}{27} - \frac{H}{2} + \left(\frac{H^2}{4} - \frac{H}{27}\right)^{\frac{1}{2}}\right]^{\frac{1}{3}} + \left[\frac{1}{27} - \frac{H}{2} - \left(\frac{H^2}{4} - \frac{H}{27}\right)^{\frac{1}{2}}\right]^{\frac{1}{3}}. \tag{9}$$

Case 2. $H < 4/27$:

Equation (7) has three real solutions, one of which is negative, say M^e_4, whereas the other two, say $M^e_5 \leq M^e_6$, are positive. The sign of the solutions of equation (7) can be controlled by using the well-known properties of the roots of a cubic equation, [1].

Case 3. $H = 4/27$:

By considering again the roots of a cubic equation we deduce immediately that (7) admits three real solutions, one negative, equal to $-1/3$, and two positive, both equal to $2/3$.

In order to study the stability of all the equilibrium solutions of system (4)–(5), we evaluate the eigenvalues $\lambda_{1,2}$ of its corresponding Jacobian matrix

$$\begin{pmatrix} c(1-2M^e) & h \\ V^e(1-V^e) & M^e(1-2V^e) - h_R U_0 \end{pmatrix},$$

and hence

$$\begin{aligned} \lambda_{1,2} &= \frac{1}{2}\left[(A+B) \pm \sqrt{(A+B)^2 + 4(K-AB)}\right] \\ &= \frac{1}{2}\left[(A+B) \pm \sqrt{(A-B)^2 + 4K}\right], \end{aligned} \tag{10}$$

where

$$A = M^e(1-2V^e) - h_R U_0, \quad B = c(1-2M^e), \quad K = hV^e(1-V^e). \tag{11}$$

First of all, since meaningful equilibrium solutions (M,V) are in the square $[0,1]\times[0,1]$, from (10) we can notice that all the eigenvalues are real: in fact, $K > 0$, for all $h > 0$. Hence, there are no focus and no Hopf bifurcations, [5].

The following two lemmas state the stability results.

LEMMA 1. *Firstly, we analyze the behavior of the solutions corresponding to* $V^e = 0$ *and* $c \geq 4h$*, for given* h_R *and* U_0*. We get:*

1. *stable nodes if* $\frac{1}{2} < M^e < h_R U_0$,
2. *unstable nodes if* $h_R U_0 < M^e < \frac{1}{2}$,
3. *unstable saddle points if* $M^e > h_R U_0$ *and* $M^e > \frac{1}{2}$ *or* $M^e < h_R U_0$ *and* $M^e < \frac{1}{2}$.

Proof. The Jacobian matrix corresponding to system (4)–(5), in this case, furnishes

$$[c(1-2M^e) - \lambda_1)](M^e - h_R U_0 - \lambda_2) = 0. \tag{12}$$

Hence, it is immediate to check that in the first case $\lambda_1 < 0$, $\lambda_2 < 0$, in the second case $\lambda_1 > 0$, $\lambda_2 > 0$ and in the third case $\lambda_1 < 0$, $\lambda_2 > 0$ or $\lambda_1 > 0$, $\lambda_2 < 0$. Hence, M_1^e is always unstable whereas M_2^e is stable (see their corresponding values in (6)), provided that its value is less than $h_R U_0$. For $c = 4h$, that is $M_{1,2}^e = 1/2$, one eigenvalue vanishes and we cannot say anything about its stability. Later on we will prove that in such a point there is a bifurcation. □

We now analyze the equilibrium solutions with values of V^e real and different from zero. In what follows we denote by λ_1 the solution corresponding to the sign minus in the r.h.s. of (10) and by λ_2 the other one.

LEMMA 2. *The solutions corresponding to* $M^e > h_R U_0$, $V^e = 1 - \dfrac{h_R U_0}{M^e}$, *and* $c \geq \frac{27}{4} h h_R U_0$, *are*

(a) unstable saddle points if $0 < M^e \leq \frac{1}{2}$,

(b) unstable saddle points if $\frac{1}{2} < M^e < \frac{2}{3}$,

(c) stable nodes if $M^e > \frac{2}{3}$.

Proof. As, in this case, $A = -M^e + h_R U_0 < 0$ and, as already noted, $K > 0$ always, then, from (10) the sign of the eigenvalues $\lambda_{1,2}$ are determined by the sign of B and $K - AB$. It is easy to check that, relative to the items of (a)–(c), we have

in (a) $B > 0$ and $K - AB > 0$, then $\lambda_1 < 0$, $\lambda_2 > 0$ for both

$A + B > 0$ and $A + B < 0$;

in (b) $B < 0$, $A + B < 0$ and $K - AB > 0$, then $\lambda_1 < 0$, $\lambda_2 > 0$;

in (c) $B < 0$, $A + B < 0$ and $K - AB < 0$, then $\lambda_1 < 0$, $\lambda_2 < 0$.

Let us note that in (b) and (c) the sign of

$$K - AB = c\,\frac{M^e - h_R U_0}{(M^e)^2}\left[\frac{h h_R U_0}{c} - (M^e)^2(2M^e - 1)\right] \tag{13}$$

is determined by the sign of the expression in the square brackets. Hence, as

$$\frac{4}{27} - (M^e)^2(2M^e - 1) = \left(\frac{2}{3} - M^e\right)\left[2(M^e)^2 + \frac{1}{3}M^e + \frac{2}{9}\right], \tag{14}$$

if $M^e > \frac{2}{3}$, then $K - AB < 0$ is satisfied because we have

$$\frac{h h_R U_0}{c} - (M^e)^2(2M^e - 1) < \frac{4}{27} - (M^e)^2(2M^e - 1) < 0. \tag{15}$$

Moreover, for $M^e = \frac{2}{3}$ one of the eigenvalues is equal to zero. Again, we will prove that for this value there is a bifurcation. □

REMARK 3. For what concerns the negative solutions $M^e_{3,4}$, in this case we have $A > 0$, $B > 0$ and $K < 0$. Thus, from (10), it is easy to check that they are unstable nodes if $(A - B)^2 + 4K > 0$ and unstable foci on the contrary. Although such solutions are not physically meaningful (also because the corresponding values of V^e become greater than one), they play, as we shall see, some role in determining the phase plane portrait of the system and its possible trend to an ecological collapse.

From the previous analysis emerges the fundamental role played by the positive parameters h, h_R, U_0 and hence from the connectivity c linked to their values. As already noted, they characterize the morphological features of the territory under study and furnish threshold values of bio-energy production in order to get a stable system. In particular, it has been shown that such a value cannot be inferior to 50% or preferable to 66.67% (under the conditions of Lemma 1 and 2, respectively) of the maximum value the environmental system can produce. Moreover, from these lemmas we see that changes in the values of these parameters produce drastic variation of the behavior of the solution that suggest to investigate about the rising of possible bifurcation phenomena. In order to carry on the bifurcation analysis, we choose as control parameter the connectivity index c also for its link to landscape fragmentation (see Appendix).

By following standard techniques, [10], we have the following lemma.

LEMMA 3. *The stationary bifurcation points of the system* (4)–(5) *are*

$$(M_1^b,\, V_1^b,\, c_1) = \left(\frac{1}{2},\, 0,\, 4h\right),$$

$$(M_2^b,\, V_2^b,\, c_2) = \left(\frac{2}{3},\, 1-\frac{3}{2}h_R U_0,\, \frac{27}{4}hh_R U_0\right).$$

Proof. By standard calculations, the stationary bifurcation points of (4)–(5) are obtained as the solutions of the following system of $2+1$ equations, [10]:

$$\begin{cases} cM - cM^2 - h + hV = 0, \\ V(M - MV - h_R U_0) = 0, \\ (M - 2MV - h_R U_0)(c - 2cM) - h(V - V^2) = 0, \end{cases} \tag{16}$$

where the third equation is obtained by equating to zero the determinant of the Jacobian matrix associated to the system (4)–(5). □

To illustrate graphically the dependence of M^e, V^e on c in a two-dimensional bifurcation diagram, we plot in two different figures, respectively, M^e and V^e solutions versus the connectivity index c. In particular in Figure 2 all the M_i^e, $i = 1,\ldots,6$ are plotted versus $c \in [0,1]$. On the contrary in Figure 3 only V_j^e, $j = 3,\ldots,6$ are reported varying $c \in [0, 4h]$, since V_1^e and V_2^e vanish for $c \geq 4h$. In the figures the values of the parameters h, h_R, U_0 correspond to a situation where $c_2 = 27hh_R U_0/4$ is less than $c_1 = 4h$.

REMARK 4. According to the results of Lemmas 1 and 2, in Figures 2 and 3 the equilibrium solutions (M_2^e, V_2^e) and (M_6^e, V_6^e) are stable, whereas the positive (M_1^e, V_1^e), (M_5^e, V_5^e) and negative (M_3^e, V_3^e), (M_4^e, V_4^e) are unstable.

We finally identify the typology of bifurcations found in Lemma 3, [5, 10].

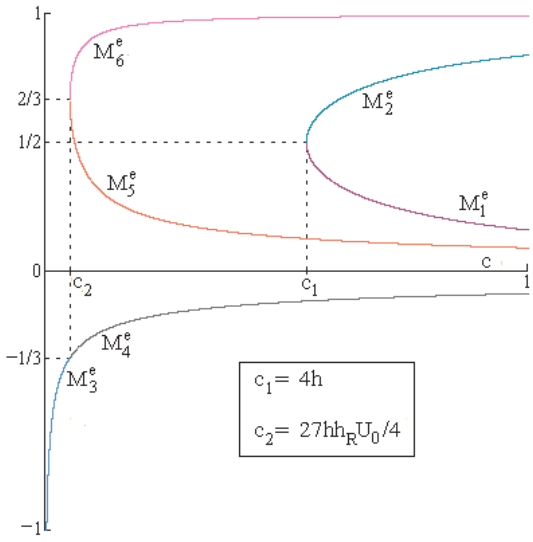

Figure 2: Bifurcation diagram of M^e versus c

LEMMA 4. *The point* (M_1^b, V_1^b, c_1) *is a simple bifurcation point, while the other one* (M_2^b, V_2^b, c_2) *is a turning or hysteresis point.*

Proof. To study the type of bifurcation, we have to evaluate the rank of the following matrix, in each stationary bifurcation point

$$G = \begin{pmatrix} c(1-2M^e) & h & M(1-M) \\ V^e(1-V^e) & M^e(1-2V^e) - h_R U_0 & 0 \end{pmatrix},$$

where the elements of the third column are the derivatives of the right-hand side of system (4)–(5) with respect to c. Being the rank of G in (M_1^b, V_1^b, c_1) not maximum, we deduce that it is a simple bifurcation point, while in the remaining point (M_2^b, V_2^b, c_2), such a rank will be equal to 2 and hence, it is candidate to be a turning or hysteresis point, where, according to Lemma 2, the superior branch is stable while the inferior one is unstable. □

REMARK 5. Note that the bifurcation diagram in Figure 2 permits to conclude immediately that the point (M_2^b, V_2^b, c_2) represents a turning point. In fact, the exchange of columns of the matrix G has a striking geometrical interpretation: rotating the diagram M^e-versus-c by $\pi/2$, the bifurcation point disappears ("turning property").

As far the point (M_1^b, V_1^b, c_1) is concerned, it is a simple bifurcation point, and in particular it is a pitchfork bifurcation. To be more precise, it is a subcritical pitchfork, because the stability is lost locally at the bifurcation point, where the superior branch is stable, whereas the inferior one is an unstable branch in agreement with Lemma 1.

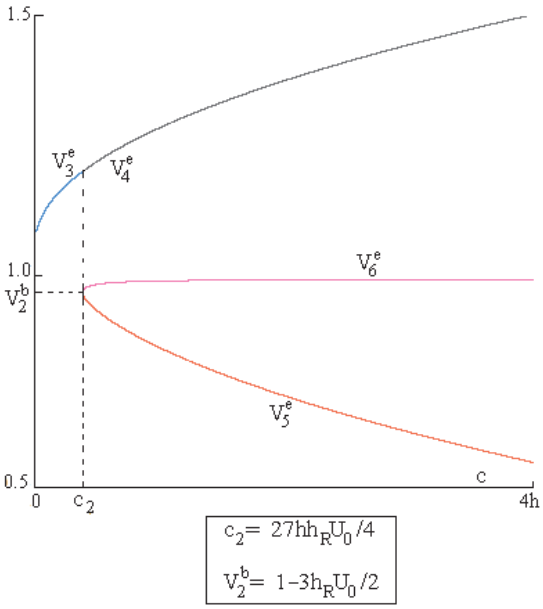

Figure 3: Bifurcation diagram of V^e versus c

REMARK 6. As already commented, for $c > \frac{27}{4}hh_RU_0$, M_5^e is unstable and M_6^e is stable. The unstable solution M_5^e (and eventually the negative unstable equilibrium M_4^e) can play an important role, for some values of c, as a repellor, so that $M \to 0$. This corresponds to an environmental system scenario where the bio-energy collapses.

In order to apply the proposed model to a real environmental system, we have considered a particular area inside the district of Cremona (already presented in Figure 1). From the ecological graph the following values of the model parameters and initial datum have been computed:

$$h = 0.655,\ h_R = 0.451,\ U_0 = 0.14,\ c = 0.481,\ P_0 = (V_0, M_0) = (0.601, 0.651).$$

With these data the condition $H < 4/27$, which assures two real positive equilibrium solutions (plus the negative one), is satisfied, and we get

$$(M_5^e, V_5^e) = (0.3692, 0.8290), \qquad (M_6^e, V_6^e) = (0.8919, 0.9292).$$

Moreover numerical calculations to determine the eigenvalues confirm that the equilibrium (M_5^e, V_5^e) is an unstable saddle point, whereas the other (M_6^e, V_6^e) is a stable node in agreement with Lemma 2. Finally, we observe that in correspondence of these values of the parameters h, h_R and U_0, the lower bound of c, which still assures the existence of the two real positive equilibria ($H < 4/27$), results to be $c = 0.2792$.

The numerical simulation of the model evolution is shown in Figure 4, where the trajectories of the system are plotted in the plane (V, M), starting from the initial

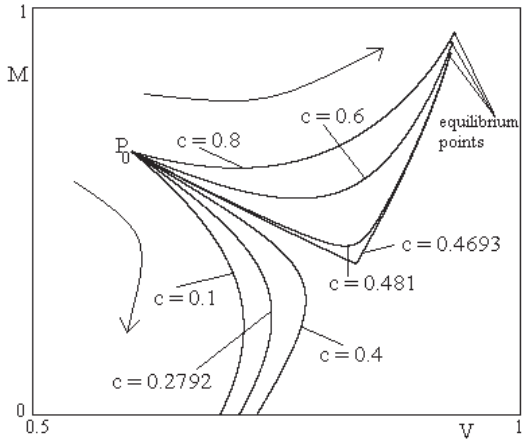

Figure 4: Phase plane portrait for different values of c

datum P_0 and varying c. The picture shows that for $c \geq 0.4693$ the system reaches asymptotically the equilibrium points (V_6^e, M_6^e). Conversely, for $c < 0.4693$ the system is repelled by the saddle-point (V_5^e, M_5^e), so that $M(t) \to 0$ and the system collapses.

In conclusion, the application shows how the system is strongly influenced by the connectivity index c. Thus, by trying to address the territorial planning in the direction of maximizing the connectivity index c, the flux of bio-energy and the level of meta-stability will be incremented, driving, hence, the territory toward a sustainable environmental development.

4. Concluding remarks

Ecological systems are complex assemblages of various biotic and abiotic components that interact among them. The study of the dynamics of such complex systems requires the use of models that simulate how they operate under the action of constraints imposed by environmental limits. For the representation of the topological space of interspecific relationships, the EG, built by means of GIS data, is a suitable mathematical tool that provides accurate information prior to a sustainable territorial planning, because it furnishes, for example, which areas must be protected and which ones improved, depending on their peculiar ecological value and, analogously, which connections must be preserved because are characterized by high energetic flux. Nevertheless, beyond a static view on graphs, fundamental questions can only be answered if dynamical analysis are also made. Structural and dynamical studies must strongly complement each other, in fact, changes in bio-energy and environmental conditions may produce territorial modifications toward which individual landscapes will tend to move smoothly (attractors) or may produce, instead, critical thresholds (bifurcation points) that modify radically the state of the ecological system.

The dynamical mathematical model that we have proposed furnishes a tool for environmental planning and management, through investigation on resistance and resilience to perturbations due to both anthropic and natural events. Equilibrium and bifurcation points furnished by the model depend on suitable values of the parameters, present in the equations, characterizing morphological features such as shape of the patch borders, permeability of barriers, bio-diversity, connectivity. In particular, the connectivity has been chosen as the control parameter, in the analysis of bifurcation, as it represents an indicator of landscape fragmentation that is an important cause of instability in modern environmental systems. Although in our mathematical model the effects of spatial scale and structure of the environment have been taken into account through the ecological graph, it would be interesting, as a future development, to introduce explicitly in our equations the spatial dependence by means of a term of diffusion [2]. An attempt in this respect has been made in [4] where the appearance of a Turing instability has been investigated.

Appendix

Let us recall that in the application to the district of Cremona (Italy), the software GIS of ESRI Arch View 3.3 was used together with the shape files that furnish information about the land uses, the presence and the connection of road infrastructures (railroads, highways, government and provincial roads), the system of water courses (natural and artificial) and the administrative subdivision of the various urban territories within the studied landscape. All this information is needed to calculate the parameters involved in the two models and that we now define.

Definition of K_j and $\mathcal{M}_{\max}$

The parameter $K_j,\ j = 1,\ldots,m$, for each patch is given by the average

$$K_j = \frac{1}{3}(K_j^S + K_j^P + K_j^D),$$

where K_j^S is a parameter which takes into account the shape of the patch borders, since their morphology influences strongly the energy exchanges between the patches themselves. Thus, it is defined by

$$K_j^S = 1 - \frac{P_j^C}{P_j} = 1 - \frac{2\sqrt{\pi A_j}}{P_j}, \qquad K_j^S \in [0,1],$$

where P_j is the perimeter of the patch j, A_j its area and $P_j^C = 2\sqrt{\pi A_j}$ the perimeter of a circle of area A_j. The above formula is constructed in such a fashion that smaller is the ratio P_j^C/P_j greater is the topological diversity of the patch with respect to a circle: such a situation of diversity is favorable to energy exchanges.

The second parameter K_j^P takes into account the permeability of the barriers, following some standard classification of values of the permeability index [3, 6], and

is given by

$$K_j^P = \frac{1}{P_j}\sum_{r=1}^{s} p_{rj}\,\ell_{rj}, \qquad P_j = \sum_{r=1}^{s}\ell_{rj}, \qquad K_j^P \in [0,1]$$

where ℓ_{rj} are the perimeter portions of P_j which have permeability index p_{rj}, $r = 1,\ldots,s$.

Finally, the third parameter K_j^D is related to bio-diversity, determined by a Shannon entropy value, that takes into account the presence of different ecotopes inside each patch. High values of bio-diversity contribute to more stable ecosystems and the parameter can be computed by

$$K_j^D = \frac{\sum_{k=1}^{H}\frac{n_k}{n}\log\frac{n_k}{n}}{\log(1/H)}, \qquad K_j^D \in [0,1]$$

where n_k is the number of ecotopes of the bio-potentiality class k between the whole number H of classes present in the patch j. Of course in the above formula the quantity $(n_k/n)\log(n_k/n)$ must be put equal to zero when $n_k = 0$.

From these definitions it should be clear that $\max\{K_j\} = 1$. Thus, we have

$$\mathcal{M}_{\max} = 2B_{\max}, \qquad B_{\max} = \max_{j=1,\ldots,m}\{B_j\} \tag{17}$$

Definition of c

In order to calculate the connectivity index c, it is necessary to define the bio-energy fluxes. These, through the border between two consecutive patches i and j, are given by

$$F_{ij} = \frac{(\mathcal{M}_i + \mathcal{M}_j)L_{ij}p_{ij}}{2(P_i + P_j)} \tag{18}$$

where L_{ij} is the length of the border, P_i and P_j are the perimeters of the two patches and p_{ij} represents the permeability index of the barrier whose value, as already said above, depends on the type of the barrier itself, [6].

The actual number of edges, and hence of the fluxes F_{ij}, depends on the chosen geographical orientation of the patches. Let us denote such a number by Λ and by F^l, $l = 1,\ldots,\Lambda$, the re-ordered values of the fluxes F_{ij}. The connectivity index is then defined as follows:

$$c = \frac{1}{\Lambda}\sum_{l=1}^{\Lambda}\frac{F^l}{\max_l\{F^l\}}. \tag{19}$$

Let us remark that, from its definition, the connectivity index c takes into account the landscape fragmentation, since the bio-energy flux through an impermeable barrier is equal to zero.

References

[1] ABRAMOWITZ M. AND STEGUN I. A. *Handbook of Mathematical Functions*. Dover, New York, 1980.

[2] CANTRELL R. S. AND COSNER C. *Spatial Ecology via Reaction-Diffusion Equations*. Wiley Series in Mathematical and Computational Biology, New York, 2003.

[3] FABBRI P. *Paesaggio, Pianificazione, Sostenibilità*. Alinea Editrice, Florence, 2003.

[4] FLAVIN J. N. AND RIONERO S. Asymptotic and other properties of a territorial bio-energy model. *Rend. Accad. Sci. Fis. Mat. Napoli 76* (2009), 95–120.

[5] GUCKENHEIMER J. AND HOLMES P. J. *Nonlinear Oscillations, Dynamical Systems and Bifurcations of Vector Fields*. Springer-Verlag, New York, 1983.

[6] INGEGNOLI V. *Landscape Ecology: A Widening Foundation*. Springer-Verlag, New York, 2002.

[7] MONACO R. AND SERVENTE G. *Introduzione ai Modelli Matematici nelle Scienze Territoriali*. Celid, Turin, 2010.

[8] NAVEH Z. AND LIEBERMAN A. *Landscape Ecology: Theory an Applications*. Springer-Verlag, New York, 1994.

[9] O'NEILL R. V., JOHNSON A. R. AND KING A. W. A hierarchical framework for the analysis of scale. *Landscape Ecology 3* (1989), 193–205.

[10] SEYDEL R. *From Equilibrium to Chaos*. Elsevier, New York, 1988.

[11] TURNER M. G. AND GARDENER R. H. *(Editors). Quantitative Methods in Landscape Ecology*. Springer-Verlag, New York, 1991.

AMS Subject Classification: 92D40, 93D20

Giuliana LAURO
Facoltà di Architettura, Seconda Università degli Studi di Napoli
Via San Lorenzo, 81031 Aversa (CE), ITALIA
e-mail: giuliana.lauro@unina2.it

Meri LISI
Dipartimento di Scienze Matematiche ed Informatiche, Università di Siena
Pian dei Mantellini 44, 53100 Siena, ITALIA
e-mail: lisi7@unisi.it

Roberto MONACO
Dipartimento di Matematica, Politecnico di Torino
Corso Duca degli abruzzi 24, 10129 Torino, ITALIA
e-mail: roberto.monaco@polito.it

Lavoro pervenuto in redazione il 21.12.2010